



Development and Characterization of Blue-Colored Mg₂Si-Based Recycled Alloys Using Scrap Light Metals

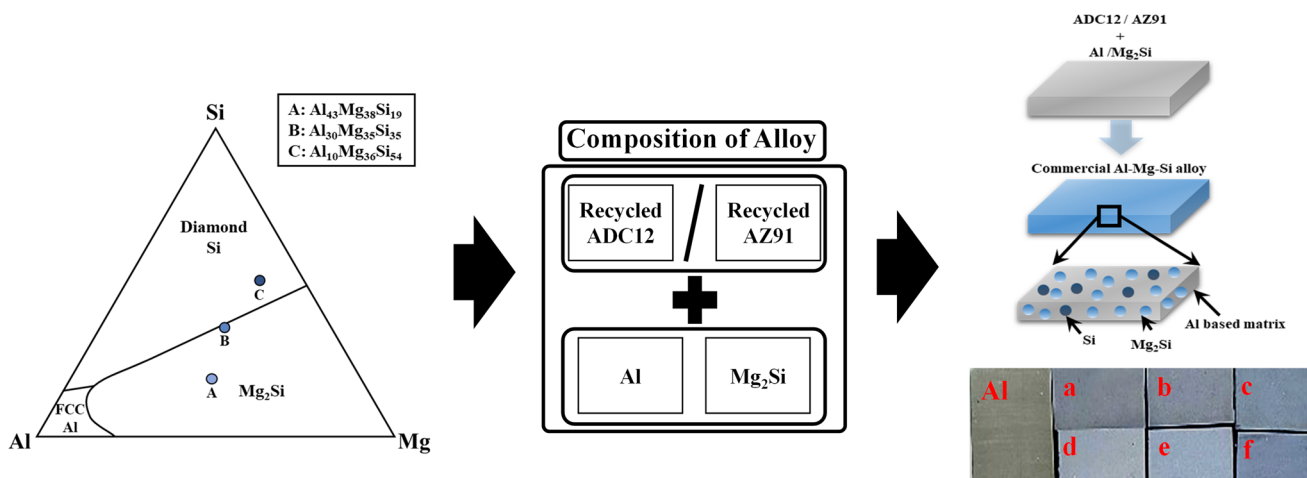
GyeolChan Kang¹ · SangChul Mun² · Hae Jin Park¹ · Sung Hwan Hong¹ · SeYoung Oh² · Kyo Chul Lee² · Ki Buem Kim¹

Received: 28 September 2021 / Accepted: 22 February 2022 / Published online: 16 March 2022
© The Minerals, Metals & Materials Society 2022

Abstract

Currently, major issues in the mobile and information and communications technology industries are consumer demands stimulated by emotion and environmental pollution issues. In the case of such consumer demand, many companies are using a demand increase model that involves the application of success stories through the convergence of design and technology, and a significant improvement has been realized. The environmental pollution caused by various dyes or resins used to realize a specific color of metal exterior materials to stimulate consumer sensibility has reached a serious level. In this study, we tried to minimize the environmental pollution that occurs due to external painting by realizing the color for the metal itself rather than through an external color coating. In addition, in the case of metal materials, the desired metal atomic ratio was similarly realized by utilizing waste scraps of the Al alloy ADC12 and the Mg alloy AZ91 that had already been used, and a study on realizing a specific color of the metal itself through recycling was conducted. Through this study, we tried to solve both environmental and consumer demand issues through recycling of metal waste materials and development of ecofriendly metal materials that do not use paint or resin.

Graphical Abstract



Keywords Commercial alloy · Color alloy · Recycled materials · CIE L*a*b* · Mg–Si–Al alloys

The contributing editor for this article was Markus Reuter.

GyeolChan Kang and SangChul Mun are co-first authors.

✉ Ki Buem Kim
kbkim@sejong.ac.kr

Extended author information available on the last page of the article

Introduction

Currently, the greatest issue in industry is the growing gap between technological development and consumer demand, and various measures are being proposed to

overcome this problem. These changes in consumer demand and technology can be confirmed through Clayton's book *The Innovator's Solution* [1]. According to Clayton, technology advances rapidly, whereas consumer demand increases relatively slowly and linearly, resulting in a gap. Since this gap becomes a factor that hinders development of technology, it must be overcome by increasing consumer demand [2, 3]. Among the methods used to increase consumer demand, the method that has proven the most effective in the mobile and information and communications technology (ICT) device industries is convergence. A synergistic effect of increasing product value through the convergence of two different fields can be created, and the increase in the value of these products compared to the production cost can have a significant impact on the increase in consumer demand. Research must be developed along the direction in which the gap between technological development and consumer demand is minimized through design-technology convergence, an example of which can be seen in how technological development and consumer demand have been realized for mobile devices through external design changes [4]. The exterior materials of mobile and electronic devices, which used to only include black, gray, and white plastic-based exterior materials, are now being implemented in various colors through metal-based exterior materials [5]. In the case of color implementation for these metal exterior materials, the surface of the metal is coated with colors using paint, resin, etc., or technology such as color implementation using anodizing or plating techniques is applied [6–9]. However, for this surface color implementation, it is realized only on the surface, resulting in poor color durability that leads to loss of color in the event of damage to the surface coating layer, such as that due to external impacts. To overcome the disadvantages of this external color implementation, this study aimed to develop colored alloys using intermetallic compounds that have their own colors [10–16]. The objective was to implement various colors through fraction control of Al using Mg_2Si , an intermetallic compound with blue color; three compositions were selected as basic compositions, and alloy development was carried out. To apply the developed alloys to the field of resource recycling, this study aimed to produce alloys similar to those produced with pure elements using waste scraps of the Al alloy ADC12 and the Mg alloy AZ91 alloys. Consumer demand can be increased and industrial problems solved by applying the concept of value-added generation through resource reuse and development of emotional materials, thus maximizing profits.

The three basic compositions made of pure elements were designed to maintain similar atomic ratios, and specimens were manufactured to perform comparative analysis of the basic compositions [14]. In addition to using the ADC12 and

AZ91 alloys with similar atomic ratios, the atomic ratio was similarly formed by adding pure elements. In the case of the basic compositions, various phases with similar chromaticity were formed to implement various changes in chromaticity and hardness due to phase interference. The alloys were designed such that only an Al-based matrix and Mg_2Si were formed in the (a) and corresponding (d) alloys in the first group, the (b) and (e) alloys in the second group were designed such that Mg_2Si and Si phases deposited in the Al matrix, and the (c) and (f) alloys in the third group were designed such that more Si phases were deposited than in the second group. The chromaticity and mechanical properties of the six alloys produced were measured, and an in-depth analysis of the chromaticity and mechanical properties of each alloy was conducted by SEM, FESEM(EDX) and TEM analysis for microstructure and phase investigation. If aluminum waste scraps are recycled based on an analysis of their mechanical properties and color differences for manufacturing of alloys using waste scraps and pure elements only, then a study can be conducted to improve the physical properties through the addition of microelements of recycled scraps. Regarding the analysis of the implemented colors, this study aimed to distinguish the colors of metals using the CIE $L^*a^*b^*$ color coordinate system, not the color-distinguishing methods of RGB, CMYK, etc. previously used [17, 18]. This system is used because of the difference in the color of the metal that exists for the color-distinguishing methods due to the glossiness of the metal itself, and the gap between the color and recognized color can be minimized by numerically expressing the glossiness to overcome this gap [19]. In the CIE $L^*a^*b^*$ color coordinate system, L^* represents luminosity in values from 0 to 100, a^* represents green and red in values from -128 to 128 , and b^* represents blue and yellow in values from -128 to 128 . A colorimetric comparison analysis using the correct tool for metal chromaticity analysis was conducted, and the colorimetric difference between the formed alloys and the color interference effect were more closely examined to analyze the colorimetric and mechanical properties of recycled metal alloys.

Experimental

The intermetallic compounds with their own colors were based on the previously developed blue magnesium silicide, which has been implemented as a suitable formulation within aluminum bases with no high solubility. Through alloy design techniques, compositions a, b, and c were all designed to form different phases, enabling analysis of various chromaticity-mechanical property correlations. To produce the representative a, b, and c composition alloys, Al (99.99 mass %, Form KRTLAB, Korea company), Mg (99.98 mass %, Form KRTLAB, Korea company), and Si

Table 1 Scrap composition and atomic ratio of developed alloys

Alloy	Atomic%								
	Mg	Si	Al	Cu	Zn	Fe	Mn	Cr	Ni
Al-AZ91	Bal.	0.02	8.15	0.01	0.23	0.01	0.08	0.01	0.01
Mg-ADC12	0.27	10.65	Bal.	0.95	0.3	0.32	0.11	0.02	0
Al–Mg–Si (AMS) A (a)	37.83	19.07	42.24	0.44	0.18	0.15	0.07	0.01	0.01
AMS B (b)	34.86	35.18	29.36	0.3	0.13	0.1	0.05	0.01	0.01
AMS C (c)	32.75	56.95	9.84	0.24	0.11	0.07	0.02	0.01	0.01
ADC-AZ A (d)	37.83	19.07	42.24	0.44	0.18	0.15	0.07	0.01	0.01
ADC-AZ B (e)	34.86	35.18	29.36	0.3	0.13	0.1	0.05	0.01	0.01
ADC-AZ C (f)	32.75	56.95	9.84	0.24	0.11	0.07	0.02	0.01	0.01

(99.999 mass %, From RNDKOREA, Korea company) were used to conduct induction casting using graphite crucibles coated with boron nitride (BN) to melt the 50 mm alloy specimen. To develop waste scrap-utilizing alloys for comparative analysis, this study aimed to manufacture alloys using waste scraps of ADC12 and AZ91 alloys.

To utilize waste of the Al alloy ADC12 and the Mg alloy AZ91, these were first cleaned using acetone and ethanol. and then, these were crushed and sieved to make particle of 3 mm diameter size. Weighing was performed to produce an alloy with a composition ratio similar to that of compositions a, b, and c so that segmented scraps had similar wt. % values. The compositions of alloys using commercial alloys and pure elements are shown in Table 1.

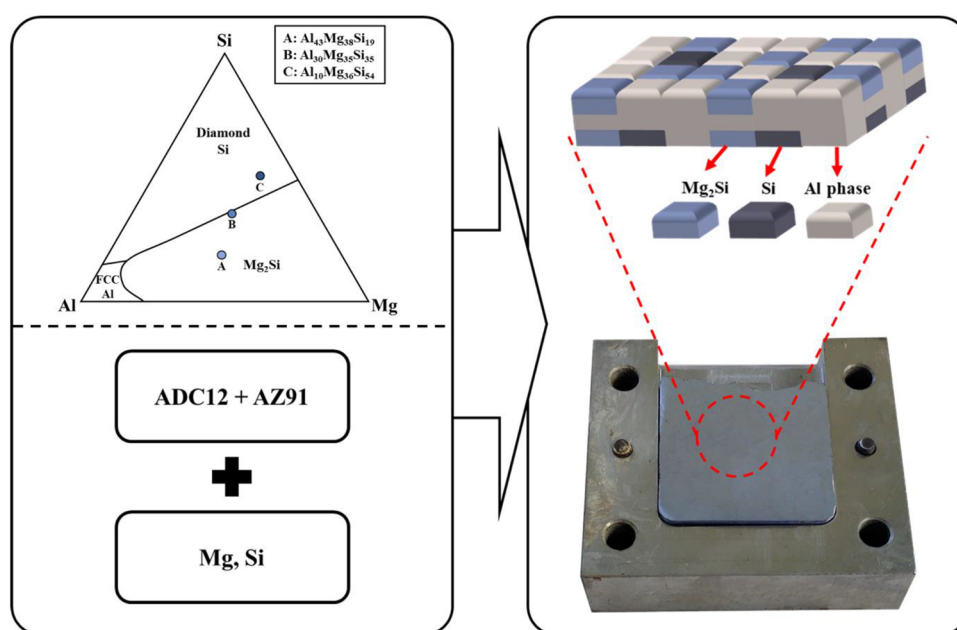
The composition groups of the alloys were set to AZ-ADC and AZ. In the AZ-ADC alloy group, ADC12 and AZ91 commercial alloys were used, and small amounts of Al, Mg and Si pure elements were added to match the three representative alloys a, b, and c. In the case of the AZ

alloy group, only AZ91 was used among the two commercial alloys, and these alloys were formed by adding small amounts of Al, Mg and Si, similar to the AZ-ADC alloy group (Fig. 1).

High-frequency induction casting was conducted under the argon atmosphere to prevent oxidation of alloy and using a carbon crucible in the casting process, and process power is about 3.5 kW and casting time is 120 s. Alloys were manufactured using plate molds of 50 mm × 50 mm × 5 mm, a specimen size of 20 mm × 10 mm × 5 mm was obtained using a high-speed cutter, and the surface of cut specimens was processed using sandpaper of 100, 400, 800, 2000, and 4000 mesh, as shown in Fig. 2.

Microstructure analysis was performed by scanning electron microscopy (SEM, JEOL JSM-6390), and energy-dispersive X-ray spectroscopy (EDX) analysis was realized by field emission scanning electron microscopy (FESEM, SU-8010). The phases of the alloys were analyzed using X-ray diffraction (XRD, Panalytical Empyrean) analysis.

Fig. 1 Basic alloy compositions according to a three-component state diagram, alloy design method using scraps, and schematic diagram of the metal and its actual implementation



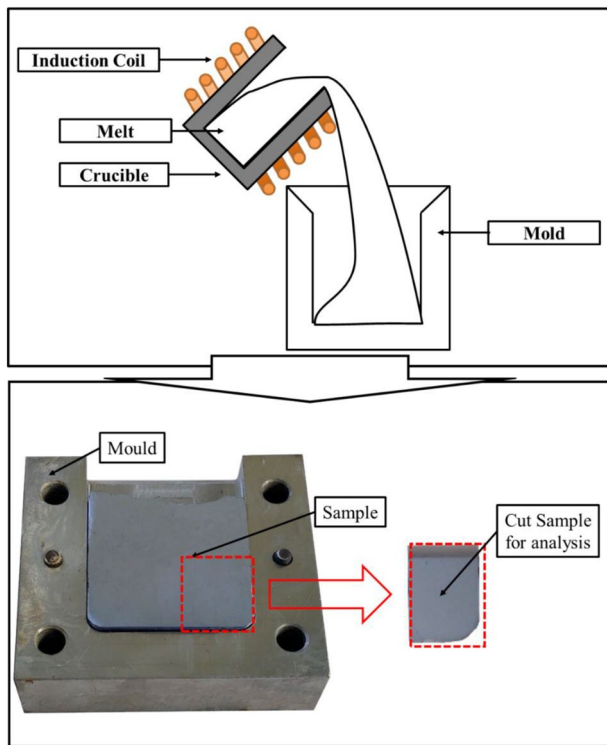


Fig. 2 Induction casting schematic diagram and photographs of a specimen produced from induction casting

Cross-section transmission electron microscopy (Cs-TEM, JEM-ARM200F) analysis was also conducted for detailed microstructure analysis. The mechanical properties of the alloys were analyzed using a micro-indenter (SHIMADZU HMV-G21DT). For chromaticity analysis of surface-treated specimens, CIE $L^*a^*b^*$ chromaticity analysis was performed through reflectance measurement of the wavelength within the visible light region using a SINCO COLOR-MATE, a photon-spectrometer instrument. The CIE color matching function was measured using the color 10° standard observer condition. The reason why the observer condition was set to 10° was that this observer condition is more suitable for color perceived by the human eye than when the observer condition is 4° , so the analysis was performed by setting the observer condition to 10° . Information about these color coordinate systems can be found in the book by Sperskaya [20]. This CIE $L^*a^*b^*$ color coordinate system is a methodology for expressing color and glossiness. Specifically, brightness can be analyzed through the L^* value, as can green through the a^* value and yellow and blue through the b^* value. CIE dE^*ab is difference value of color with the target metal. When it has more than 2.4 value, we can decide color difference. Also, d^*a and d^*b parameters are difference value of a^* and b^* , respectively. For the color coordinate values measured in this study, the L^* and a^* values do not produce significant changes in chromaticity, so the analysis

of chromaticity changes and mechanical property changes was based on a comparative analysis of b^* values. Mg_2Si and Si phases that are close to blue are expected to have a significant impact on the b^* value.

A comparative analysis of surface hardness was performed using the Vickers hardness test on polished surfaces of plate-shaped specimens of $20\text{ mm} \times 10\text{ mm} \times 5\text{ mm}$ produced through the fabrication and preparation of specimens to analyze the mechanical properties. The compression condition was set at 5 N and maintained for 10 s; the position of the indenter was changed, and 10 times repeated analysis each sample were performed. An electronic densimeter was used to analyze the density, and the measurements were carried out on each specimen using the hydrometer technique under 20° atmospheric conditions.

Results and Discussion

The color implementation for metals using intermetallic compounds was performed following the juxtaposition technique, in which colors are combined according to the colors formed by each microstructure, and their combination is seen as a single color [21, 22]. In this study, various color improvements were conducted through phase fraction control via compositional control such that the color implementation varied through changes in the fractions and forms of the Mg_2Si phase, Si single phase, and colorless Al-based mixture phase. According to a previous study, the smallest size that can be discerned by the human eye is $20 \sim 330\ \mu\text{m}$, and in the case of metal, when the microstructure has this characteristic, the overall color appears uniform and homogeneous [14, 23]. The microstructure of the alloys developed in this study is a combination of the Mg_2Si phase and the remaining Al-based matrix and Si phase, and except for in the a and b compositions, the Mg_2Si and Si phases are formed in many sizes from 10 to $100\ \mu\text{m}$. Similar shapes are observed in the microstructure of alloys manufactured using waste scraps; the d, e, and f alloys corresponding to the a, b, and c alloys show similar microstructures to each corresponding alloy. The following Fig. 3 shows microstructure images of the alloy compositions manufactured in this study, showing no significant difference in phase size or fraction between the a, b, and c alloys using pure elements and d, e, and f alloys using waste scraps, along with similar microstructure shapes.

Through this, the ability to obtain results similar to those of alloys produced using pure elements when producing blue alloys using waste scraps was confirmed, and an XRD analysis test was conducted to check the consistency of each phase of the microstructures. The XRD analysis results showed that compositions a and d contained α -Al

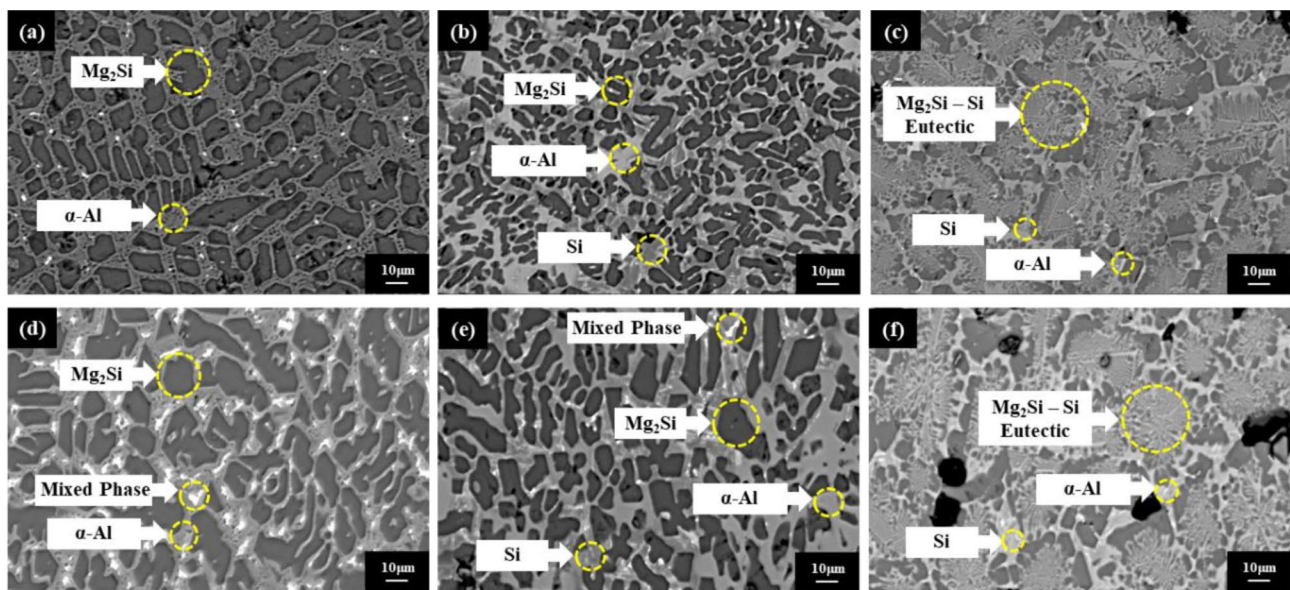
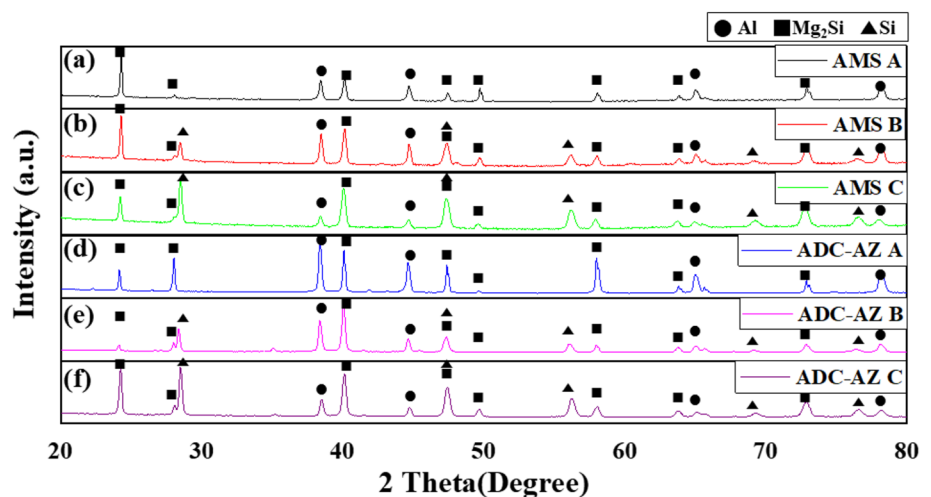


Fig. 3 $\times 500$ Magnification SEM images of alloys developed in this study. **a** AMS A, **b** AMS B, **c** AMS C, **d** AZ-ADC A, **e** AZ-ADC B, and **f** AZ-ADC C alloys

and Mg_2Si phases, but in the case of compositions b, c, e, and f, diamond_A4 silicon phases were formed in addition to the $\alpha-Al$ and Mg_2Si phases, Fig. 4. Furthermore, the microfractional elements contained in the scrap were confirmed to form additional mixed phases when making alloys using waste scraps. Through this, the development of alloys using waste scraps similar to existing alloys was confirmed, and the similarity of alloys was verified through in-depth microstructure and phase analysis. The XRD analysis results are shown in the following Fig. 4 to confirm that other phases were formed that cannot be identified from the microstructure alone. The XRD analysis results were consistent with the microstructure analysis results. This means the existence of $\alpha-Al$, Mg_2Si and Si phase.

These results also confirmed that alloys similar to conventional alloys can be formed by casting using waste scraps. The results of EDX analysis to perform composition and phase analysis of microunits are shown in the following Fig. 5, as the addition of microelements does not exclude the possibility of results different from the XRD analysis results. Except for the d composition, the EDX results show that phases similar to those in the XRD analysis results are formed for the compositions; the Mg_2Si phase and Si phase are formed separately, and the Al phase is also formed. However, the d composition shows different results from the previous experimental results in the polar microstructure, and some of the microstructure shows the presence of phases formed by mixing of aluminum and magnesium.

Fig. 4 XRD patterns of alloys developed in this study. (a) AMS A, (b) AMS B, (c) AMS C, (d) AZ-ADC A, (e) AZ-ADC B, and (f) AZ-ADC C alloys



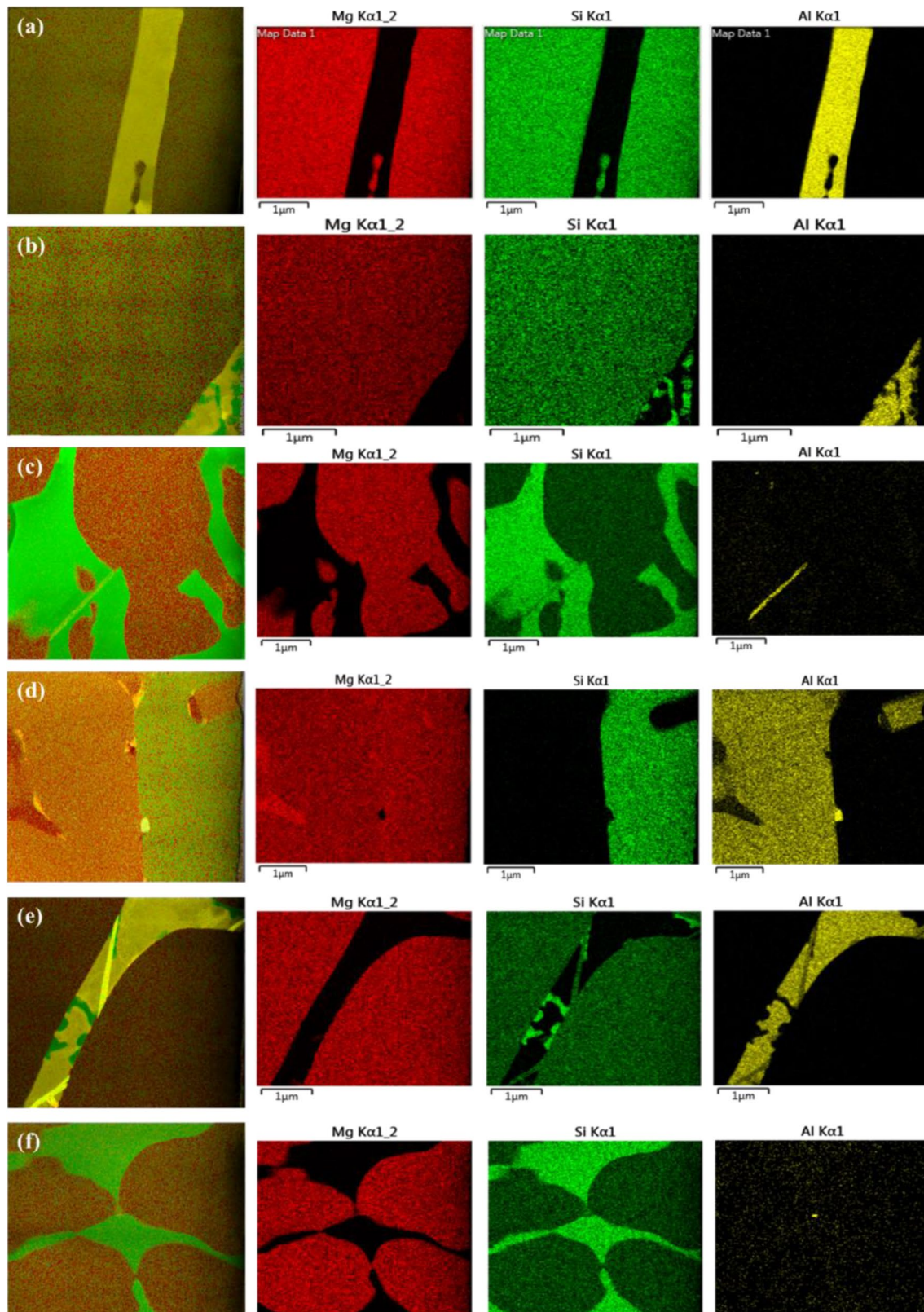


Fig. 5 EDX images of alloys developed in this study. the image show content of element Al (yellow), Mg (red) and Si (green). **a** AMS A, **b** AMS B, **c** AMS C, **d** AZ-ADC A, **e** AZ-ADC B, and **f** AZ-ADC C alloys (Color figure online)

The formation of these Al–Mg alloys can be attributed to the formation of Al–Mg alloys and to the formation of Mg_2Si , as microelements such as Cr, Mn, Fe, Ni, Cu, and Zn present in waste scraps act as nucleation sites [24, 25]. Compositional analysis of all developed compositions showed that the d, e, and f alloys developed using waste scraps were very similar to the previously developed a, b, and c alloys in terms of microstructure and phase structure. However, in alloy d, additional Al–Mg phases were formed, and the effect of these additional phases on the chromaticity and mechanical properties must be determined. Through a clear analysis of the mechanical properties and chromaticity of the formed Al–Mg, accurate prediction of chromaticity and mechanical property changes and control of them enable the desired color or mechanical properties of the study to be implemented. To this end, a clear analysis method of the structures of the formed phases must be presented, and in this study, analysis of the phases formed in the alloy was performed through TEM analysis. The composition a TEM results showed that only 110 zone axis aluminum and 001 zone axis Mg_2Si phases were formed, as targeted in the alloy design, and that only fractional effects of the aluminum and Mg_2Si phases existed. The mechanical properties are also expected to differ in terms of hardness depending on the ratio of phases formed according to the level rule, and factors that enhance the mechanical properties such as eutectic structures are unlikely to be measured [26–28]. In the case of composition b, unlike composition a, the Si phase was also observed, and each phase was a 111 zone axis Mg_2Si phase, a 110 zone axis Al phase, or a 110 zone axis Si phase. Composition c shows the three phases of Al, Mg_2Si , and Si similar to composition b, and the TEM analysis showed no difference compared to composition b. However, composition d differed from the previously developed alloys, and the analysis of the phases showed that the 101 zone axis Mg_2Si phase and the 111 zone axis Al phase were the same as those in alloy a, but additional 112 zone axis $Al_{140}Mg_{89}$ and 112 zone axis $Mg_{17}Al_{12}$ phases were observed [26, 29, 30]. For composition e, there was no significant difference from composition b, but for composition f, there were a few aluminum phases, unlike composition c, which was expected to show only Mg_2Si and Si phases (Fig. 6).

These microstructure and phase analysis results confirm that similar alloys are formed, but if there are significant differences in chromaticity and mechanical properties, as in this study, then a comparative analysis of chromaticity and mechanical properties is required. Thus, comparative analysis of chromaticity using CIE $L^*a^*b^*$ color coordinate analysis and hardness using Vickers indentation was performed. The chromaticity analysis of the $Al_{140}Mg_{89}$ and $Mg_{17}Al_{12}$ (β) phases formed in the d composition showed that the $-b^*$ values, corresponding to the blue chromaticity, were 2.29 and 1.76, respectively. These are similar to

the $-b^*$ value of -2 corresponding to the existing blue color diagram of aluminum, and the lack of change in chromaticity is likely due to the formation of a new phase that replaces the aluminum phase. However, the presence of fractional variations of Mg_2Si through the formation of phases containing Mg results in chromatic variations due to color differences between Mg_2Si ($-b^*:13$) and Si ($-b^*:5$); thus, chromatic analysis of all compositions was conducted to closely observe the chromatic variations according to phase formation. The results of this chromaticity analysis are shown in Table 2.

According to the chromaticity analysis by composition, the L^* value representing glossiness does not have a significant effect on the implementation of chromaticity, and it was excluded when measuring the chromaticity in this study, which tends to vary with surface hardness. In addition, in the case of the a^* values representing red and green, the chromaticity difference is not noticeably large, so distinguishing the chromaticity variation of the blue metal implementation using only the b^* values is reasonable. The results of chromaticity and hardness measurements for each composition are shown in the graph in Fig. 7b. The chromaticity and hardness analysis shows that the blueness of the commercial alloy-based manufactured alloys corresponding to compositions a, b, and c is much higher than that of compositions d, e, and f. The difference is predicted to be due to the action of microelements used in commercial alloy scraps, such as d. These changes in phase and microstructure may result in changes in the fraction, size and shape of the Mg_2Si or Si phase with a specific color, which may result in changes in the overall color. Increases in the overall sizes of the Mg_2Si phase and the Si phase result in a difference in color reflectance, which can be determined to be a successful improvement in the physical properties through recycling, and the possibility of replacing the pure element alloy with an alloy containing waste scrap can be discussed.

As can be seen Fig. 7a, Analysis of the mechanical properties shows that the hardness values of the d and e compositions are similar but slightly lower than those of the a and b compositions, which are associated with the mechanical properties decreasing as the phase size increases due to the Hall–Petch effect. However, in the case of the c and f compositions, significant differences in the mechanical properties occur, which can be thought to be due to volume fraction difference between Mg_2Si and Si phases, about 5% increase Mg_2Si phase at f composition compared to c composition, except for the eutectic structures. This can be expected to result from the soft properties of aluminum, which contrasts with the high hardness of Mg_2Si intermetallic compounds and Si phases, and composition f containing relatively large amounts of microelements does not have time to form a separate aluminum phase. The results of this study show that both good chromaticity and hardness can be achieved in

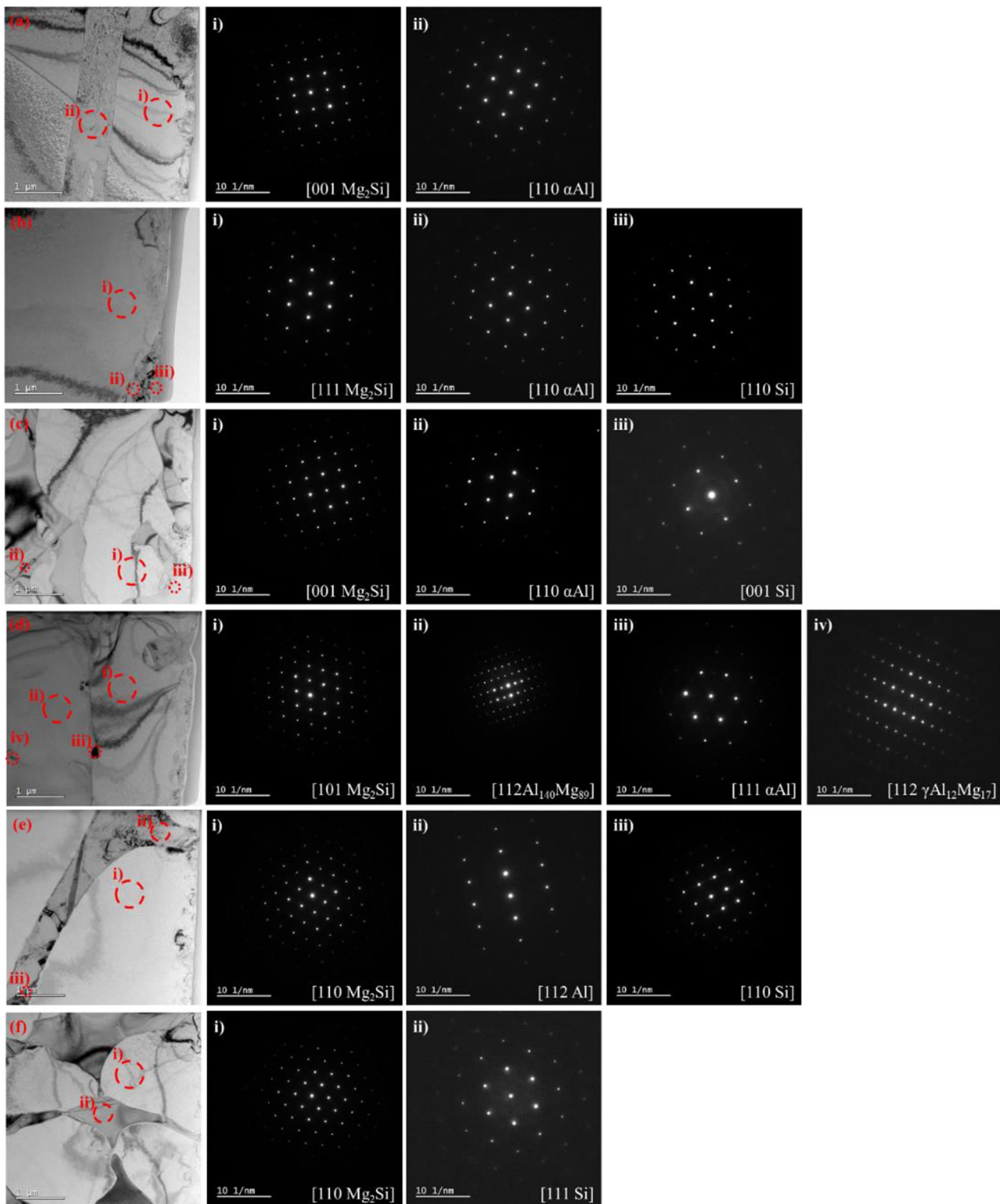


Fig. 6 TEM images of alloys developed in this study. **a** AMS A, **b** AMS B, **c** AMS C, **d** AZ-ADC A, **e** AZ-ADC B, and **f** AZ-ADC C alloys

alloys manufactured using waste scraps compared to alloys manufactured using existing pure elements, along with similar or better mechanical properties. However, if alloys are

produced using these waste scraps, then consideration of the manufacturing price is inevitable. Although there is an advantage of reducing environmental costs when recycling

Table 2 Comparison analysis of chromaticity and color differences by composition

Composition #	Mg ₂ Si (Target)	A(AMS a)	b(AMS b)	c(AMS c)	D(AZ-ADC a)	e(AZ-ADC b)	f(AZ-ADC c)
L*(brightness)	75.12	71.51	69.11	62.92	81.84	78.26	73.83
a*(yellowness)	-1.31	-0.10	-0.27	-0.59	-0.83	-0.96	-1.01
-b*(blueness)	13.13	4.70	6.30	8.35	6.91	7.68	9.50
CIE dE*ab (color difference)	0.00	11.92	12.73	16.90	13.12	8.79	4.94
d*a (yellowness difference)	0.00	0.10	0.27	0.59	0.83	0.96	1.01
d*b (blueness difference)	0.00	8.43	6.83	4.78	6.22	5.45	3.63
Color							

resources, whether manufacturing costs are reduced when using actual waste scraps must be confirmed, along with the gains from these abstract concepts. To this end, this study aimed to perform a benefit–cost ratio (BCR) analysis. The BCR represents the benefit of an investment compared to the cost, expressed by the following ratio [31].

$$BCR = \frac{\text{Program benefits}}{\text{Program cost}}$$

The purpose of this BCR analysis was to compare only the costs of the elements because the alloy compositions developed in this study had the same manufacturing method; therefore, the cost comparison according to manufacturing cost was meaningless. For the alloys produced using existing pure elements, the reference value was set at 1, and for the alloys produced using waste scraps, the BCR values were 1.81, 1.35, and 1.17 for compositions d, e and f, respectively.

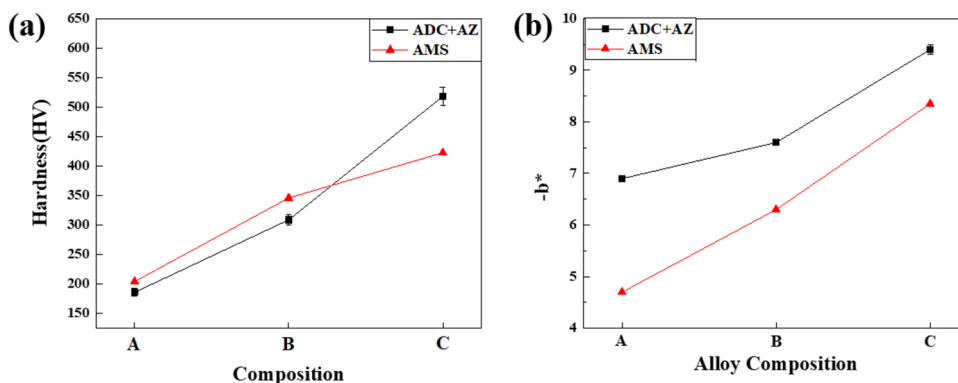
Table 3 Benefit cost comparison analysis between alloys manufactured using pure elements and alloys manufactured using scrap

Composition	A (a, d)	B (b, e)	C (c, f)
BCR			
AMS	1	1	1
ADC-AZ	1.81	1.35	1.17
Price (\$/100 g)			
AMS	37.4	49.7	64.3
ADC-AZ	30.5	44.9	62.7

These BCR analysis results and element prices per 100 g are shown in Table 3 below.

Through this, the use of waste scraps in all compositions can be judged to be beneficial, and considering the reduction in environmental costs through recycling, a great benefit is expected. Chromaticity and mechanical properties are likely

Fig. 7 Comparative analysis of the **a** hardness and **b** chromaticity of alloys manufactured using AMS colored alloys and scraps



to be realized at the desired level through recycling, and the scope of application for the development of colored alloys can likely be expanded.

Conclusions

This study aimed to develop an alloy with its own color using waste scrap, and the method of developing the alloy involved adding 40 weight percent of Mg and Si elements compared to total composition to the waste scrap and maintaining a similar ratio to the existing composition, and implement the alloy with the desired color. In addition, overall color control of the alloy was possible by adjusting the phases of the alloy through control of the alloy composition. When comparing the a, b, and c alloys, the Mg₂Si volume fraction did not show much difference at the about 50%, and the overall color and properties of the alloys changed due to the influence of the Si single phase according to the composition change. The AZ-ADC and AZ alloy groups showed better blueness than the previously developed AMS alloys and did not show significant differences in terms of mechanical properties. This result is thought to be due to the influence of the additional elements in the commercial alloys, but accurately analyzing the mechanism is difficult because there are too many variables by composition. The alloys of this study can be used in various applications, such as in metallic material design, as vehicle exterior materials, and as electronic device exterior materials, and they are expected to enable the realization of more various colors than previously developed alloys. In addition, commercial alloys are widely used throughout industry and have many manufacturing processes, and they have the advantage of a lower cost than pure metal materials requiring purification. When comparing the costs of manufacturing AMS alloys using pure metal elements and AMS alloys using commercial alloys, the manufacturing of alloys using commercial alloys developed in this study was less expensive. The ability to recycle waste scraps and scraps from the manufacturing process of commercial alloys is also expected.

Acknowledgements This research was supported by the Bio & Medical Technology Development Program of the National Research Foundation (NRF) and the Korea Institute of Radiological and Medical Science (KIRAMS) funded by the Korean government (MSIT) (2021M2E7A1079168, 50461-2021). It was supported by the National Research Foundation of Korea (NRF) and the grant was funded by the Korean government (NRF-2018R1A2B3007167)

Declarations

Conflict of interest The authors declare that they have no known competing financial interests or personal relationships that could have appeared to influence the work reported in this paper.

References

- Christensen C, Raynor M (2013) *The innovator's solution: Creating and sustaining successful growth*. Harvard Business Review Press, Boston
- Triberti S, Chirico A, La Rocca G, Riva G (2017) Developing emotional design: emotions as cognitive processes and their role in the design of interactive technologies. *Front Psychol* 8:1773
- Zhou F, Ji Y, Jiao RJ (2021) Emotional design. In: *Handbook of human factors and ergonomics*, 5th edn. Gavriel Salvendy and Waldemar Karwowski, John Wiley & Sons, Inc., pp 236–251
- Akay D, Kurt M (2009) A neuro-fuzzy based approach to affective design. *Int J Adv Manuf Technol* 40(5–6):425
- Longley WV (1995) Automotive color certification. *Color Res Appl* 20(1):50–54
- Runge J (2014) Anodizing for design and function. *J Mater Sci Nanotechnol* 1(7):S108
- Runge JM (2018) *The metallurgy of anodizing aluminum*. Springer, Cham
- La-Niece S (2013) *Metal plating and patination: cultural, technical and historical developments*. Elsevier, Amsterdam
- Mattox DM (2000) Ion plating—past, present and future. *Surf Coat Technol* 133:517–521
- Wolff IM (2002) Precious metal compounds. In: *Intermetallic compounds: principles and practice: progress*, vol 3, pp 53–84
- Steinemann S, Wolf W, Podloucky R (2002) Color and optical properties. *Intermet Compd-Princ Pract* 3:231–244S
- Hong SH, Mun SC, Kang GC, Park HJ, Jeong YB, Song G, Kim KB (2022) Recent development of coloring alloys. *Prog Mater Sci* 123:100811
- Barnes C (1984) The coloration of metals. *Rev Prog Color Relat Top* 14(1):127–131
- Mun SC, Kang GC, Jeong YB, Park HJ, Kim YS, Hong SH, Song G, Kim KB (2021) Development of coloring alloys: color design for lightweight Al-mg-Si alloys. *Mater Des* 200:109449
- Jeong YB, Hong SH, Kim JT, Park HJ, Kim YS, Lee HD, Lee JK, Mun SC, Hwang YJ, Heo K (2018) Investigation on the relationship between transition energy and the color change of Cu–M alloys. *Met Mater Int* 25:539–545
- Jeong YB, Hong SH, Park HJ, Kim YS, Kim JT, Lee HD, Hwang YJ, Lee YH, Kim KB (2018) Investigation of color change in Cu–Zn alloys by reflectivity and color difference analysis. *Korean J Metals Mater* 56(3):171–176
- Hoffmann G (2003) Cielab color space. <http://www.fho-empden.de/~hoffmann/cielab03022003.pdf>
- Hunter R (1948) Accuracy, precision, and stability of new photoelectric color-difference meter. In: *Journal of the Optical Society of America*, vol 12, Amer Inst Physics Circulation Fulfillment Div, 500 Sunnyside Blvd, Woodbury, pp 1094–1094
- Gonnet J-F (1998) Colour effects of co-pigmentation of anthocyanins revisited—1. A colorimetric definition using the CIELAB scale. *Food Chem* 63(3):409–415
- Speranskaya N (1959) Determination of spectrum color coordinates for twenty-seven normal observers. *Opt Spectrosc* 7:424–428
- Seo S, Yoon K (2010) Color juxtaposition for pointillism based on an artistic color model and a statistical analysis. *Vis Comput* 26(6–8):421–431
- Sørensen BM (2014) *The method of juxtaposition: Unfolding the visual turn in organization studies*. The Routledge companion to visual organization. Routledge, Milton Park, pp 66–83
- Na JH, Han KH, Garrett GR, Launey ME, Demetriou MD, Johnson WL (2019) Designing color in metallic glass. *Sci Rep* 9(1):3269

24. Janudom S, Rattanochaikul T, Burapa R, Wisutmethangoon S, Wannasin J (2010) Feasibility of semi-solid die casting of ADC12 aluminum alloy. *Trans Nonferr Met Soc China* 20(9):1756–1762. [https://doi.org/10.1016/S1003-6326\(09\)60370-8](https://doi.org/10.1016/S1003-6326(09)60370-8)
25. Furuta S, Taniguti K, Kobayashi M, Aoba T, Miura H, Aoyama S, Uesaka N (2019) Relationship between changes in X-ray measured residual stress and inhomogeneity of microstructure in heat-treated of ADC12 alloy die-castings. *J Jpn Foundry Eng Soc (Online)* 91(6):335–342
26. Calvert L, Villars P (1991) *Pearson's handbook of crystallographic data for intermetallic phases*. ASM International, Materials Park
27. Han J, Kim K, Yi S, Park J, Sohn S, Kim T, Kim D, Das J, Eckert J (2008) Formation of a bimodal eutectic structure in Ti–Fe–Sn alloys with enhanced plasticity. *Appl Phys Lett* 93(14):141901
28. Song GA, Han JH, Kim TE, Park JM, Kim DH, Yi S, Seo Y, Lee NS, Kim KB (2011) Heterogeneous eutectic structure in Ti–Fe–Sn alloys. *Intermetallics* 19(4):536–540. <https://doi.org/10.1016/j.intermet.2010.11.030>
29. Braun R (2006) Investigation on microstructure and corrosion behaviour of 6XXX series aluminium alloys. In: *Materials science forum*, vol 519. Trans Tech Publications Ltd, pp 735–740
30. Mezbahul-Islam M, Mostafa A, Medraj M (2014) Essential magnesium alloys binary phase diagrams and their thermochemical data. *J Mater*. <https://doi.org/10.1155/2014/704283>
31. Devarakonda S (2019) Calculating the economic viability of corporate trainings (traditional & elearning) using benefit-cost ratio (BCR) and return on investment (ROI). *Int J Adv Corp Learn* 12(1):41–57

Publisher's Note Springer Nature remains neutral with regard to jurisdictional claims in published maps and institutional affiliations.

Authors and Affiliations

GyeolChan Kang¹ · SangChul Mun² · Hae Jin Park¹ · Sung Hwan Hong¹ · SeYoung Oh² · Kyo Chul Lee² · Ki Buem Kim¹

¹ Department of Nanotechnology and Advanced Materials Engineering, Sejong University, 209 Neungdong-ro, Gwangjin-gu, Seoul 05006, Republic of Korea

² Division of RI-Convergence Research, Korea Institute of Radiological & Medical Science, 75 Nowon-ro, Nowon-gu, Seoul 01812, Republic of Korea